

AD-A207 540

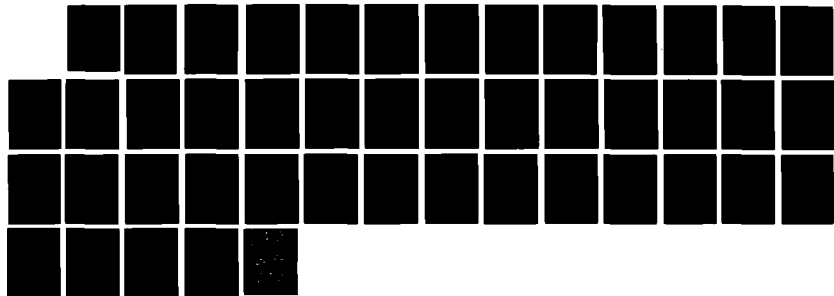
NONLINEAR ATTENUATION MECHANISM IN SALT AT MODERATE  
STRAIN BASED ON SALMO. (U) MISSION RESEARCH CORP SANTA  
BARBARA CA G D MCCARTOR ET AL DEC 88 HRC-R-1204  
AFGL-TR-89-0013 F19628-87-C-0240

1/1

UNCLASSIFIED

F/G 19/11

NL





AFGL-TR-89-0013

**AD-A207 540**

**Nonlinear Attenuation Mechanism in Salt  
at Moderate Strain Based on Salmon Data**

**G. D. McCartor  
W. R. Wortman**

**Mission Research Corporation  
735 State Street  
P.O. Drawer 719  
Santa Barbara, CA 93102**

**December 1988**

**Scientific Report No. 3**

**Approved for public release; distribution unlimited**

**AIR FORCE GEOPHYSICS LABORATORY  
AIR FORCE SYSTEMS COMMAND  
UNITED STATES AIR FORCE  
HANSCOM AIR FORCE BASE, MASSACHUSETTS 01731-5000**

DTIC  
ELECTE  
MAY 5 1989  
S A D

89 5 5 066

Sponsored by:

DARPA Order No.

Monitored by:

Contract No.

Defense Advanced Research Projects Agency

Nuclear Monitoring Research Office

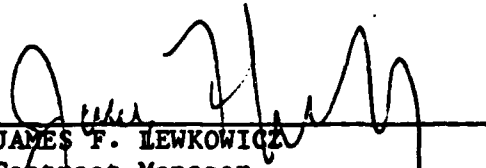
5307


Air Force Geophysics Laboratory

F19628-87-C-0240

The views and conclusions contained in this document are those of the authors and should not be interpreted as representing the official policies, either expressed or implied, of the Defense Advanced Research Projects Agency or the US Government.

"This technical report has been reviewed and is approved for publication"

  
JAMES F. LEWKOWICZ  
Contract Manager  
Solid Earth Geophysics Branch  
Earth Sciences Division

  
JAMES C. BATTIS  
Acting Chief  
Solid Earth Geophysics Branch  
Earth Sciences Division

FOR THE COMMANDER

  
DONALD H. ECKHARDT, Director  
Earth Sciences Division

This document has been reviewed by the ESD Public Affairs Office (PA) and is releasable to the National Technical Information Service (NTIS).

Qualified requestors may obtain additional copies from the Defense Technical Information Center. All others should apply to the National Technical Information Service.

If your address has changed, or if you wish to be removed from the mailing list, or if the addressee is no longer employed by your organization, please notify AFGL/DAA, Hanscom AFB, MA 01731-5000. This will assist us in maintaining a current mailing list.

Do not return copies of this report unless contractual obligations or notices on a specific document requires that it be returned.

Unclassified

SECURITY CLASSIFICATION OF THIS PAGE

1.2.4.207 540

Form Approved  
OMB No. 0704-0188  
Exp. Date: Jun 30, 1985

## REPORT DOCUMENTATION PAGE

1a. REPORT SECURITY CLASSIFICATION Unclassified			1b. RESTRICTIVE MARKINGS		
2a. SECURITY CLASSIFICATION AUTHORITY			3. DISTRIBUTION/AVAILABILITY OF REPORT Approved for public release; distribution unlimited		
2b. DECLASSIFICATION/DOWNGRADING SCHEDULE					
4. PERFORMING ORGANIZATION REPORT NUMBER(S) MRC-R-1204			5. MONITORING ORGANIZATION REPORT NUMBER(S) AFGL-TR-89-0013		
6a. NAME OF PERFORMING ORGANIZATION Mission Research Corporation	6b. OFFICE SYMBOL (if applicable)		7a. NAME OF MONITORING ORGANIZATION Air Force Geophysics Laboratory		
6c. ADDRESS (City, State, and ZIP code) 735 State Street, P.O. Drawer 719 Santa Barbara, CA 93102-0719			7b. ADDRESS (City, State, and ZIP code) Hanscom Air Force Base Massachusetts 01731-5000		
8a. NAME OF FUNDING/SPONSORING ORGANIZATION	8b. OFFICE SYMBOL (if applicable)		9. PROCUREMENT INSTRUMENT Identification NO. F19628-87-C-0240		
8c. ADDRESS (City, State, and ZIP code)			10. SOURCE OF FUNDING NUMBERS		
			PROGRAM ELEMENT NO. 62714E	PROJECT NO. 7A10	TASK NO. DA
11. TITLE (Include Security Classification) Nonlinear Attenuation Mechanism in Salt at Moderate Strain Based on Salmon Data					
12. PERSONAL AUTHOR(S) G. D. McCartor; W. R. Wortman					
13a. TYPE OF REPORT Scientific #3	13b. TIME COVERED From_ To_		14. Date of Report (Year, Month, Day) 1988 December		15. PAGE COUNT 44
16. SUPPLEMENTARY NOTATION					
17. COSATI CODES			18. SUBJECT TERMS (continue on reverse if necessary and identify by block number) Salmon Nonlinear Attenuation Partial Shear Failure		
FIELD	GROUP	SUB-GROUP			
19. ABSTRACT (Continue on reverse if necessary and identify by block number) In order to describe the seismic pulse or source function from UGTs outside the region of nonlinear attenuation, data from the Salmon event (5.3 kT in salt) have been examined to serve as the basis for a description of a mild nonlinear attenuation mechanism. It is found that a precursor in the Salmon pulses can be attributed to a partial shear failure of the medium which operates above a compressional strain threshold of about $10^{-4}$ . When this loss mechanism is included along with a linear Q of about 10, the Salmon pulses in the moderate strain regime are nearly reproduced in both amplitude and shape. Using this result the pulse can be propagated out to a range for which no further shear failure occurs and it can serve as a linear source function. <i>Corrected for 3</i>					
20. DISTRIBUTION AVAILABILITY OF ABSTRACT <input type="checkbox"/> Unclassified/Unlimited <input checked="" type="checkbox"/> Same as RPT. <input type="checkbox"/> DTIC Users			21. ABSTRACT SECURITY CLASSIFICATION UNCLASSIFIED		
22a. NAME OF RESPONSIBLE INDIVIDUAL James Lewkowicz			22b. TELEPHONE (Include Area Code) (617) 377-3028		22c. OFFICE SYMBOL AFGL/LWH

DD FORM 1473, 84 MAR

83 Apr edition may be used until exhausted.

SECURITY CLASSIFICATION THIS PAGE

All other editions are obsolete

Unclassified

## TABLE OF CONTENTS

Section	Page
1 INTRODUCTION . . . . .	1
2 MODERATE STRAIN ATTENUATION DATA IN SALT . . .	3
3 MECHANISM FOR SALMON ELASTIC PRECURSOR . . .	6
4 COMMENTS . . . . .	17
REFERENCES . . . . .	19
Appendix	
A WILKINS FINITE DIFFERENCE EQUATIONS . . . . .	A-1
REFERENCES . . . . .	A-5
B INCLUSION OF DAY-MINSTER Q IN FINITE DIFFERENCES . . . . .	B-1
REFERENCE . . . . .	B-4

## LIST OF ILLUSTRATIONS

Figure	Page
1    Salmon radial velocity pulses seen at 166, 225, 276, 318, 402 and 660 meters range (time zero on plot corresponds to initial signal arrival at 166 meters which was at 0.036 seconds after detonation) . . . . .	7
2    Calculated pulses at Salmon ranges for pure plastic medium . . . . .	8
3    Stress-strain curve for partial shear failure . . . . .	11
4    Calculated pulses at Salmon ranges for shear failure . . . . .	12
5    Cowboy Q estimates as a function of peak strain . . . . .	13
6    Calculated pulses at Salmon ranges for shear failure and $Q=10$ . . . .	15
7    Calculated pulses at Salmon ranges for smoothed shear failure and $Q=10$ . . . . .	16
B-1 Absorption band Q and propagation speed C for three values of the Padé index m for $Q_0 = 20$ , $\tau_1 = 1.59 \times 10^{-3}$ and $\tau_2 = 1.59 \times 10^{-1}$ . .	B-3

## SECTION 1

### INTRODUCTION

In order to characterize a distant seismic pulse according to the energy which generated it, a source function<sup>1</sup> is needed which can be used to initiate the seismic signal at sufficient range from the event that the subsequent propagation can be described in *linear* terms according to the properties of the earth. Thus an observed seismic signal implies a source function which may be compared with known functions for discrimination and yield estimation. Therefore, the properties of such source functions must be known to use this technique. Near-field data from various events have been taken. The smallest strains observed, due to practical free field instrument placement selection, are typically no less than  $10^{-5}$  and are often much greater. If the pulse at this extreme range undergoes no further significant nonlinear modification, its characterization can supply the needed source function. However, if any additional nonlinear changes are important, a useful source function cannot be determined. Consequently, it is important to characterize any possible nonlinear attenuation of moderate strain pulses, preferably through methods which allow generalization to all placement media of interest.

There is a long history of development of numerical methods for calculation of strongly nonlinear behavior in the near field of UGTs.<sup>2,3</sup> The gross nonlinear effects of vaporization, crushing, cracking and plastic behavior induced by strains much greater than  $10^{-3}$  must be taken into account to obtain an understanding of near field data taken at NTS. Complex equations of state or constitutive relations including effective stress and porosity are needed for a description.<sup>4</sup> These methods generally apply for strains greater than  $10^{-3}$ ; at lesser strains linear behavior is assumed. However, as indicated in the following section, it seems clear that some residual nonlinear effects continue out to strains less than  $10^{-5}$ . Ideally one would like to have a physically based model of any nonlinear effects in order to use existing near field data to define a more distant linear source function or at least to determine what effect, if any, the nonlinearities over the moderate strain range have on the linear source function.

In order to determine this, we are attempting to develop nonlinear constitutive relations for the mildly nonlinear attenuation in the moderate strain regime (scaled ranges of  $10^2$  m/kT<sup>1/3</sup> to  $10^4$  m/kT<sup>1/3</sup> or strains from  $10^{-3}$  to  $10^{-6}$ ) for explosively generated seismic pulses. The relations are to be used to determine the character of seismic pulses in the linear low-strain regime (beyond  $10^4$  m/kT<sup>1/3</sup>) which may then



serve as source functions for regional or teleseismic propagation. A linear source function can be found by numerical propagation of an experimentally well known initial pulse through the moderate strain range to account for mild nonlinear attenuation.

Experimental data provide significant restrictions on candidate constitutive relations. Attenuation in a salt medium from Salmon,<sup>5-10</sup> Cowboy,<sup>11-13</sup> Livermore small scale explosions,<sup>14</sup> Rockwell damped oscillation experiments<sup>15</sup> and New England Research ultrasonic pulse attenuation,<sup>16</sup> with one exception, are fairly consistent internally. The first three provide a detailed indication of the change of amplitude and shape of explosively driven pulses. Proposed constitutive relations must reproduce these data. The data from the wide range of yields in salt indicate that yield<sup>1/3</sup> scaling applies with a remarkable precision; if all times and distances are scaled by yield<sup>1/3</sup>, the scaled amplitudes and shapes of pulses from all experiments are nearly the same.<sup>17</sup> Thus the initial pulse on entering the moderate strain regime must scale at some small scaled range and the subsequent attenuation must result from constitutive relations which have no time or space scales which are fixed by the medium. This provides a significant reduction in the domain of allowable nonlinear behavior. For example, the relations may be a function of the strain but they may not depend on the strain rate.

In order to investigate nonlinear constitutive relations, a standard numerical time stepping method is used. The technique which we have used is that of taking the observed Salmon initial velocity pulse at small range (166 meters) as a source and comparing the resulting pulses as they are propagated through material subject to candidate constitutive relations. The results are compared with observed signals at larger ranges. For any constitutive relation the *effective Q* associated with the attenuation may be determined but it must be emphasized that nonlinear attenuation cannot be properly described by a *Q* function; still *Q* may sometimes be useful for comparison with past work. The fundamental comparison of the data with calculations is not in terms of the *Q* but in terms of reproduction of waveform including both amplitude and shape.

## SECTION 2

### MODERATE STRAIN ATTENUATION DATA IN SALT

The most comprehensive attenuation data, over the range of moderate strains, exists in the medium of salt. For explosive sources the laboratory results of Larson<sup>14</sup> covers strains from  $10^{-1}$  to  $10^{-3}$ , the Salmon field test<sup>5</sup> covers strains for  $10^{-3}$  to  $10^{-4}$  while the Cowboy field test<sup>11</sup> series covers strains from  $10^{-4}$  to  $10^{-5}$ . The Rockwell<sup>15</sup> laboratory decaying oscillations complete the salt data by ranging from  $10^{-5}$  to  $10^{-8}$ . The NER<sup>16</sup> laboratory ultrasonic pulse propagation experiments go from less than  $10^{-6}$  to more than  $10^{-5}$ . The essential results of these experiments will now be reviewed.

Larson's laboratory data were taken from the effects of a series of small chemical explosives in blocks of pressed salt. Velocity data were taken at several gauges such that the totality of the examples from all shots covered peak velocity to compressional velocities, which is approximately the peak strain, of  $10^{-1}$  to  $10^{-3}$ . Using a triplet of records from a single shot, it was estimated that over peak strains of  $1.4 \times 10^{-3}$ ,  $7.0 \times 10^{-4}$  and  $4.6 \times 10^{-4}$ , the  $Q$  changes from 12.5 to 24.9. The corner frequency for this small scale experiment was about  $5 \times 10^4$  Hertz.

The Salmon data were generated by a 5.3 kT nuclear explosion in salt. The work by McCartor and Wortman<sup>7</sup> as well as McLaughlin and Gupta<sup>8</sup> shows that the high quality data clearly indicate a high level of attenuation. It is estimated that for peak strains from  $4 \times 10^{-3}$  to  $3 \times 10^{-4}$ , the effective  $Q$  is to order of 10 at a corner frequency of about 6 Hertz. This  $Q$  appears nearly constant,<sup>7</sup> perhaps increasing mildly with range,<sup>8</sup> over the order of magnitude strain range available. However, in view of the fact that small strain data from other experiments, including the decoupled event Sterling<sup>8</sup> which used the Salmon cavity, indicate a much larger  $Q$ , it seems likely that there are residual nonlinearities at the extreme range of the Salmon data so that  $Q$  must increase at larger ranges (and so smaller strains).

Tittmann<sup>15</sup> has studied the attenuation of flexural and torsional harmonic oscillations of salt samples. It has been found that the attenuation, expressed in terms of  $Q^{-1}$  as a function of strain amplitude, tends to be nearly constant for strains from  $10^{-8}$  to  $10^{-6}$ , then increase for greater strains. The attenuation is a decreasing function of confining pressure with an average  $Q$  of approximately 200 at  $10^{-6}$  strain at a frequency of 400 Hertz for confinement consistent with the explosions.

Rockwell Elastic Properties, Finite Deformation

The regime covered by the COWBOY experiments overlaps that for Salmon, by beginning at strains of about  $5 \times 10^{-3}$  and extending out to  $10^{-5}$ . The COWBOY experiments consisted of a series of shots over a range of yields, both coupled and uncoupled, such that the individual events generally had only a few instruments in operation. Several authors have combined these data by invoking the experimentally compelling evidence for simple scaling, which suggests that the velocity pulse data from various yields can be equated by scaling all times and distances by the cube root of the yield. This is particularly dramatic when peak velocity is plotted against scaled range giving a consistent curve over about ten orders of magnitude in yield. Larson has pointed out that the full velocity pulses, as well as their peak values, tend to be preserved through scaling.

Trulio<sup>10</sup> has analyzed the scaling-combined Cowboy data to estimate  $Q$  as dictated by decrease in peak displacement with range by using one decade at a time in the frequency domain. He has found that attenuation decreases as range increases in a fashion inconsistent with linearity expressed as dispersive harmonic potential waves. If the coupled Cowboy data are fit assuming a  $Q$  independent of range (a possibility due only to scatter in the data),  $Q$  must be a function of frequency ranging from about 5 at low frequencies (1 Hz at Salmon scale) to nearly 100 at high frequencies (32 Hz at Salmon scale). However, simple scaling is inconsistent with this fit since scaling requires linearity coupled with a  $Q$  independent of frequency. If the decay of the reduced displacement potential is fit by the form  $\exp(-\omega r/2cQ)$ , it is seen that simple scaling can result so long as, for constant  $c$ ,  $Q$  is a function of a variable which is unchanged by scaling – such as  $\omega r$ . Trulio has shown that the a range of data from Salmon, through Cowboy and Cowboy Trails, do have the property that an effective  $Q$  can be expressed as a function of  $\omega r$  for all the experiments. Obviously this indicates that at fixed frequency, the attenuation expressed in terms of  $Q$ , is dependent upon range. Since it is assumed that the medium is approximately homogeneous, the implication is clear that the attenuation must be amplitude dependent and so nonlinear.

Minster and Day<sup>12</sup> have used the scaled peak velocity data for COWBOY to determine if these data require an amplitude (nonlinear) or frequency dependent  $Q$  for consistency. They determined that a  $Q^{-1}$  which consists of a small constant (consistent with small strain data from Tittmann) plus a term proportional to the peak strain provides a good fit to the data. The observed attenuation effects do not firmly indicate the need for a frequency dependent  $Q$  but indicate that an amplitude dependent  $Q$  provides a more convincing fit than a constant  $Q$ . Based on the small strain  $Q$ , which is several hundred as seen in the Rockwell experiments, it is concluded that there must be nonlinear attenuation in the COWBOY strain regime.

Coyner<sup>16</sup> of New England Research has carried out a series of laboratory experiments for which compressional and shear ultrasonic pulses consisting of about two cycles at 100-200 kHz were propagated through a sample. Attenuations were calculated using a spectral ratio technique. Variation of the attenuation with peak strain amplitude and confining pressure were determined. Experiments were carried out with several materials including Sierra White Granite, Berea Sandstone and Dome Salt. For the dome salt it was found that over a strain range of  $5 \times 10^{-7}$  to  $3 \times 10^{-6}$  and for a confining load range of 0.1 to 1 MPa, the P-wave attenuation is nearly constant and can be described by a Q of about 20. There is no particular evidence of nonlinearity in these data alone.

In summary, the salt data appear to support the hypothesis that explosively generated pulses encounter nonlinear attenuation for strains much greater than  $10^{-6}$ . No detailed knowledge of the attenuation mechanism currently exists but there does appear to be a consistency in that the explosively generated pulses closely obey simple scaling which suggests that the mechanism must be rate independent. The *effective* Q for this process increases with increasing frequency and increases with decreasing strain. In the next section we shall attempt to exploit a feature of the Salmon near-field pulses which suggests a physical mechanism which can account for the attenuation data.

### SECTION 3

#### MECHANISM FOR SALMON ELASTIC PRECURSOR

The Salmon data have a feature which may be useful in understanding some nonlinear effects of attenuation. Each of the pulses experimentally observed at six sensors at ranges from 166 meters to 660 meters exhibit a discontinuity in the slope upon the initial steep rise in pulse velocity, as seen in Figure 1. This appears as a toe-like behavior in the leading edge of the velocity profile which has been described by Perret<sup>5</sup> as an "elastic precursor" to the main pulse. The absolute amplitude of the toe remains approximately constant with range, at a particle velocity of about 0.5 m/s, while its amplitude relative to the peak increases with range. This precursor amplitude corresponds to a compressional strain level of  $\epsilon \approx 10^{-4}$ . The leading edge of the pulses (i.e., that disturbance earliest in time) propagates at a speed of about 4.7 km/sec while the pulse peaks, always after the toe, propagate at a speed of about 3.7 km/sec. The elastic compressional speed of mild disturbances in this salt medium found from independent measurements is typically about 4.6 km/sec. This indicates that the precursor signal seen in the Salmon data is due to elastic behavior while the subsequent pulse suffers a lower propagation speed due to some relaxation or plastic behavior. If propagation were purely plastic the sequence of pulses seen at the Salmon sensor sites would be as shown in Figure 2.

Perret suggests an elastic-plastic material behavior might account for the data in perhaps one of two ways. First, the precursor could develop at large strain, where an elastic limit is exceeded from radii much smaller than instrumented for Salmon, and continue to propagate in front of a following plastic wave. Second, it may be that the precursor develops in the moderate strain region if dome salt has an elasto-plastic nature at such strains. In either case, the modulus of salt must be a function of the strain - that is, the medium is nonlinear.

If the precursor develops at large strain there must be an elastic limit beyond which plastic behavior provides a lower modulus. When such a medium is dynamically loaded beyond the elastic limit, a leading pulse at the elastic limiting stress is generated followed by a larger amplitude but slower plastic wave. If the elastic-plastic transition is not sharply defined, the resulting pulse could consist of a gently rising leading elastic front which smoothly merges with the main plastic pulse much as seen in the Salmon data. Perret points out that if some energy from the plastic component is fed to the elastic portion during propagation, the amplitude of the elastic piece

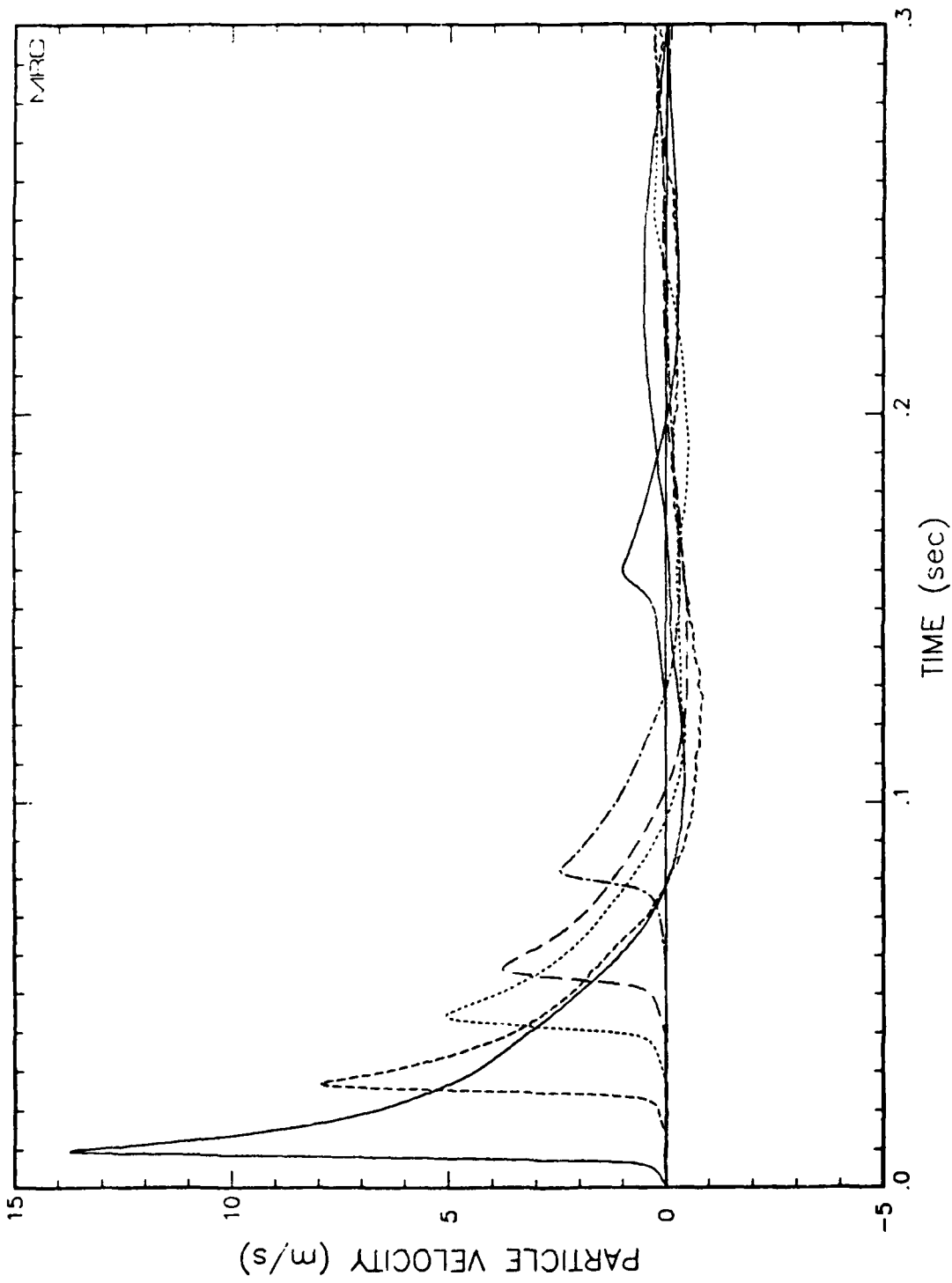


**Figure 1.** Salmon radial velocity pulses seen at 166, 225, 276, 318, 402 and 660 meters range (time zero on plot corresponds to initial signal arrival at 166 meters which was at 0.036 seconds after detonation).

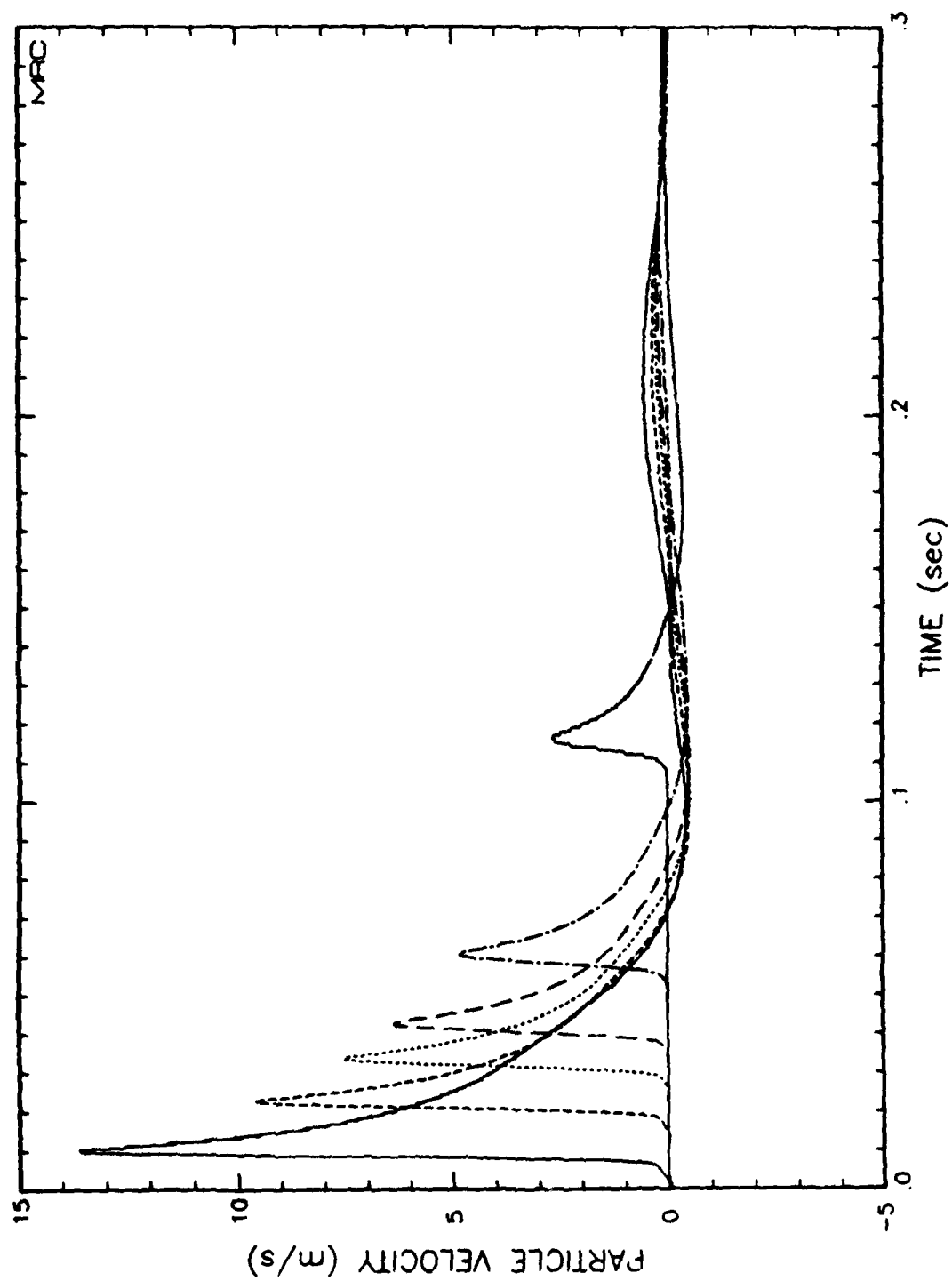


Figure 2. Calculated pulses at Salmon ranges for pure plastic medium.

could remain nearly constant, but this is quite speculative. What is known is that a variety of laboratory experiments show that strong impulsive sources can produce elastic precursors in a variety of media. For example, work of Ahrens and Duvall<sup>18</sup> with planar pulses in quartz generated by explosives exhibits an apparent elastic stress limit of about 70 kbar corresponding to strains of about  $10^{-1}$ . This produces a leading edge, described as the elastic shock, which propagates at a speed in excess of that of the deformational portion of the pulse which follows. The elastic shock propagates with an equivalent modulus which is greater than the static modulus at this high stress. It is speculated that the elastic wave is supported by a higher than equilibrium shear stress. After the elastic component has passed, the shear stress is apparently reduced to the static value by a plastic or fracture process. This experiment as well as others<sup>19</sup> which show an elastic precursor consistent provide elastic limits of many or tens of kilobars in contrast with the Salmon data which gives a precursor amplitude of about 5 bars. Consequently this mechanism does not seem a likely means of accounting for the Salmon data which give a nearly constant and small precursor amplitude which seems to begin near the 166 meter sensor range rather than be well developed by this time.

The second possibility indicated by Perret is that of having the precursor develop locally in the observation region based on moderate strain plastic behavior. While there is no accepted dynamical equation of state for dome salt, Perret points out that dome salt is known to be highly plastic - under static conditions, it is nearly hydrostatic. Thus plastic deformation of salt at moderate stresses is apparently normal. In order to account for the precursor data in Salmon, the equation of state would have to provide linear behavior up to a threshold (a threshold of about 5 bars, much less than the 70 kbars found for the elastic shock discussed above) and through some deformation of the material, relax the modulus abruptly (on the Salmon time scale) to a value which provides a compressional propagation speed about 20% less than for infinitesimal strains in undisturbed material. Having a threshold at the observed and nearly constant precursor amplitude avoids having to account for the constancy of the precursor by arguments of convenience about feeding energy back from the plastic portion of the wave.

As an equation of state model which can be consistent with the Salmon data, consider a medium for which the shear modulus permanently (that is, does not recover until the pulse is past) decreases upon having a critical strain threshold exceeded; the compressional modulus before and after exceeding the strain threshold reflects the compressional speeds at the beginning and peak of the Salmon pulses, respectively. This will be referred to as a shear failure model. Depending upon the relation between the compressional and shear moduli, complete shear failure may occur, meaning that



the elastic shear modulus,  $\mu$ , goes to zero. For the example used in this discussion, the compressional speed decreases to 80% of its original value. We have taken the Lamé constants  $\lambda$  and  $\mu$  to have a ratio of 2. Thus a decrease of the compressional speed,  $((\lambda + 2\mu)/\rho)^{1/2}$ , where  $\rho$  is the density, of 20% corresponds to reducing  $\mu$  to about 38% of its elastic value when  $\lambda$  is held fixed. Note that the reduction of modulus at a fixed strain is consistent with scaling since the strain is a unitless quantity and there is no rate dependence. The scaling restriction does require that the relaxation time of the modulus change be short compared with any representative time scale of the data; we take the transition to be instantaneous. Figure 3 indicates the stress-strain curve which results from this model for the modulus. In order to determine the effect on the pulse propagation we used the observed Salmon velocity at 166 meters as the source. The calculations were carried out using a standard finite difference methods whose details are provided in Appendix A.

As an initial effort, the elastic threshold was taken at a compressional strain of  $10^{-4}$ ; the resulting pulse sequence at the ranges to observation stations for Salmon is as shown in Figure 4. Note that the character of the calculated precursor is much like that seen experimentally, in Figure 1, in that the leading feature is drawn out, the transition to the main pulse takes place at a constant amplitude and the peak now moves at a significantly lower speed. Still the amplitude of the main peak does not decrease as quickly as the data indicate.

When the modulus decreases, the elastic energy in the pulse also decreases in a manner approximately proportional to the square of the compressional wave speed. Since the modulus reduction is permanent, this energy is lost to the pulse and goes into heating the medium. For the parameter used, over a full cycle for which most of the pulse exceeds the critical strain, approximately one-third of the original elastic energy will be lost. This corresponds to an effective  $Q$  of about 13 for peak strains well in excess of  $10^{-4}$  (for small strains less than this threshold, there will be no loss). This value of  $Q$  is far less than that expected for very small strains but it is still more than the 5 to 10 seen for Salmon attenuation. The addition of a moderate level of linear attenuation consistent with that seen for small to moderate strains in other experiments will improve the agreement (for example, the NER data suggest  $Q \approx 20$ ). More importantly, the use of a partial shear failure mechanism will automatically terminate once the pulse weakens so that the peak strain falls below the critical strain threshold value. This will produce a sharply changing effective  $Q$  in a manner suggested by the Cowboy data as given in Figure 5. Thus this first attempt to reproduce the Salmon data is encouraging but there remain differences which may be accounted for by refining the details of the attenuation mechanism.

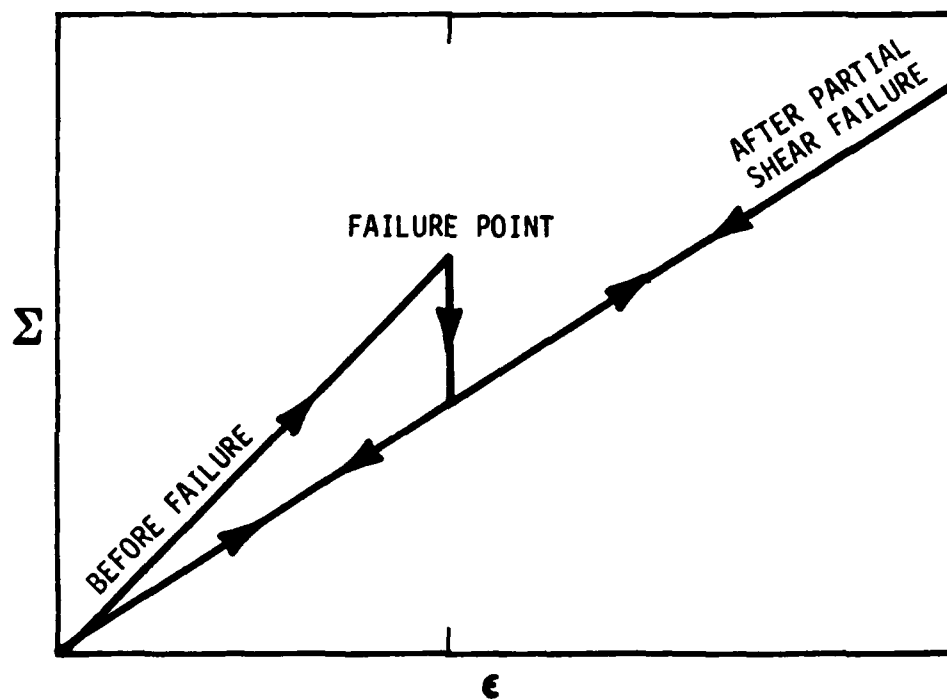


**Figure 3. Stress-strain curve for partial shear failure.**

SALMON FROM QF 166-660

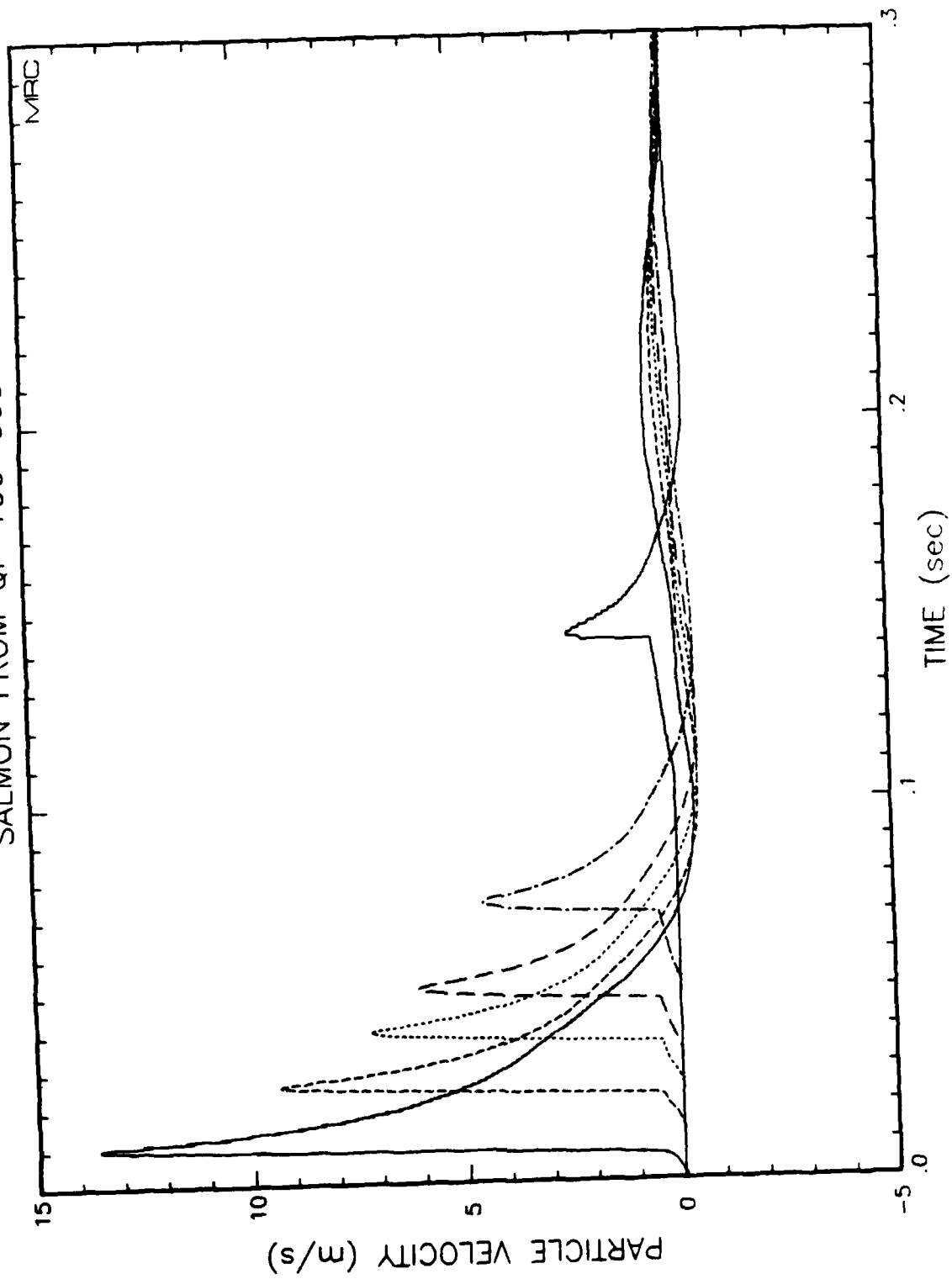


Figure 4. Calculated pulses at Salmon ranges for shear failure.

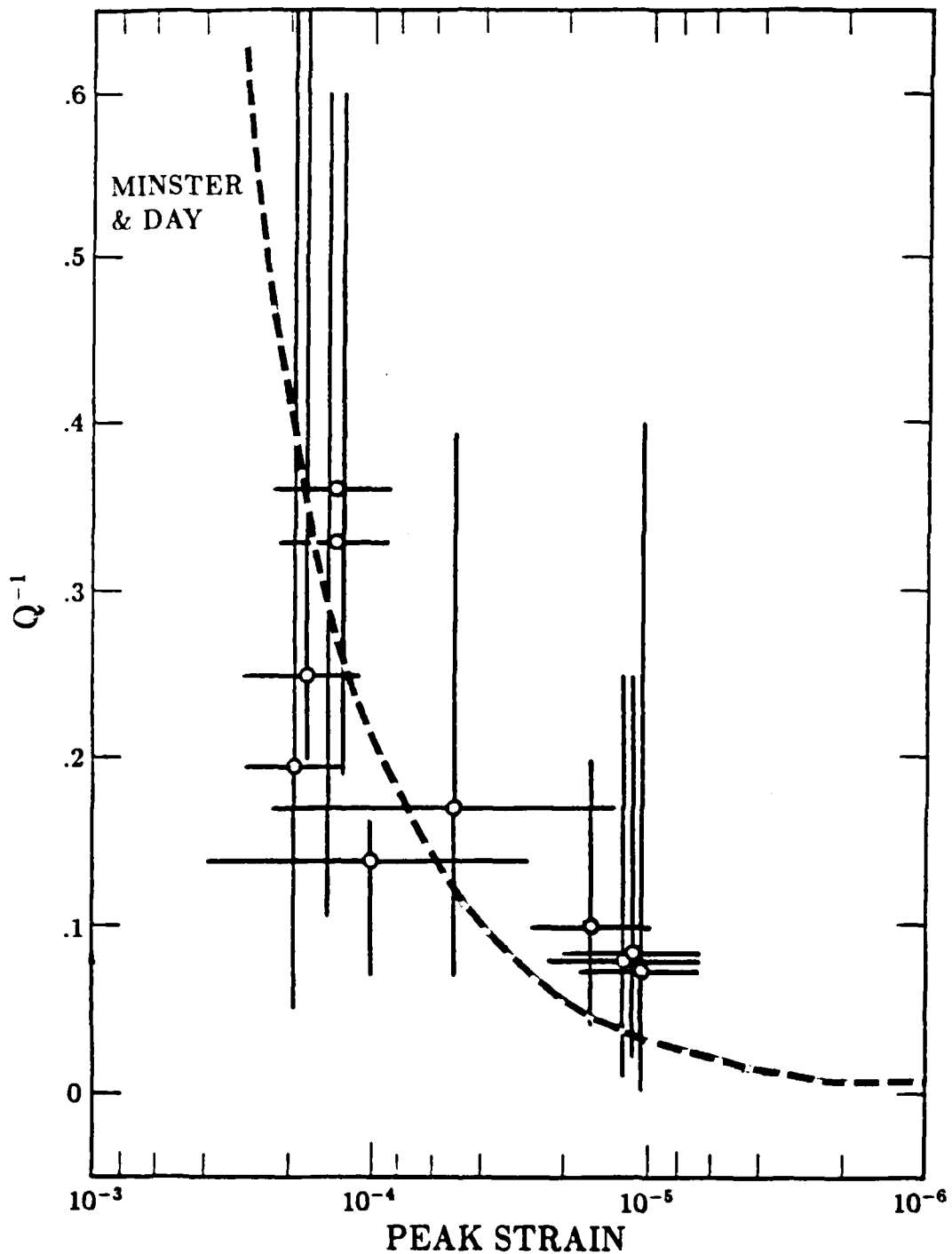


Figure 5. Cowboy  $Q$  estimates as a function of peak strain. The horizontal bars represent the two record strain values while the vertical bars indicate the spread of  $Q$  over a decade of frequency. The fit of Minster and Day is provided. (From Ref. 13).

The attenuation from partial shear failure does not produce an amplitude for the pulse at 660 meters which is as small as that seen experimentally. More attenuation can be added to attempt to match better the data by employing a linear  $Q$  of sufficient value. A method of inclusion of a linear absorption band  $Q$  in time stepping finite difference methods has been demonstrated by use of Padé approximants. Our application of this method is outlined in Appendix B. This formalism was employed using a target  $Q$  of 10 with a range of half amplitude frequencies of 1 to 100 Hertz ( $Q$  rises above 20 beyond these values). The sequence of pulses which result using both the partial shear failure and a linear  $Q$  of 10, starting with the Salmon pulse at 166 meters, is shown in Figure 6. The amplitudes for the main peaks now are in substantial agreement with the data and the length and amplitude of the precursor are also reproduced fairly well. Still there remains a very abrupt transition from precursor to main pulse which is clearly sharper than the experimental data.

One further refinement has been applied to the partial shear failure model in order to avoid the abrupt transition between precursor and pulse. Since there is certain to be a range of material properties even in the relatively homogeneous salt dome, it is reasonable to require a range of thresholds for the shear failure. The model has been altered to produce a variation of failure threshold values of compressional strain over a range of 30% with a constant probability about the  $10^{-4}$  value. Each cell in the finite difference calculation is given its own threshold which is randomly drawn on this basis. The set of pulses at the Salmon instrument ranges then calculated is given in Figure 7. The result is a smoother transition from precursor to main pulse in a manner which is quite similar to the actual Salmon data shown in Figure 1. While it is probably possible to achieve a detailed fit to the data by further such refinements, this is not a very meaningful thing to do since the mechanisms are not understood to the required level of detail. The important point is that it is possible to reproduce the data to a substantial degree using only a few physically based parameters.

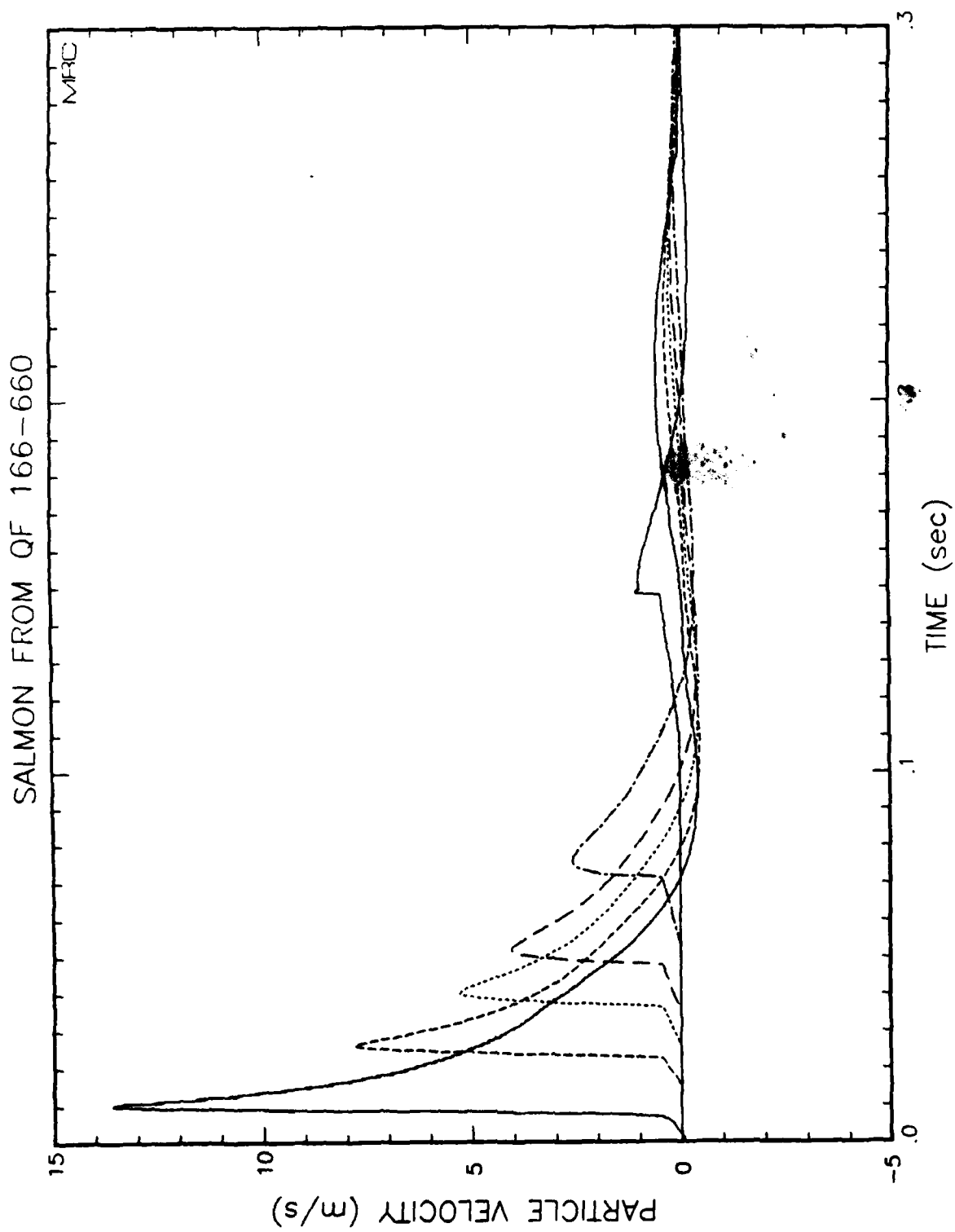


Figure 6. Calculated pulses at Salmon ranges for shear failure and  $Q=10$ .

SALMON FROM QF 166-660

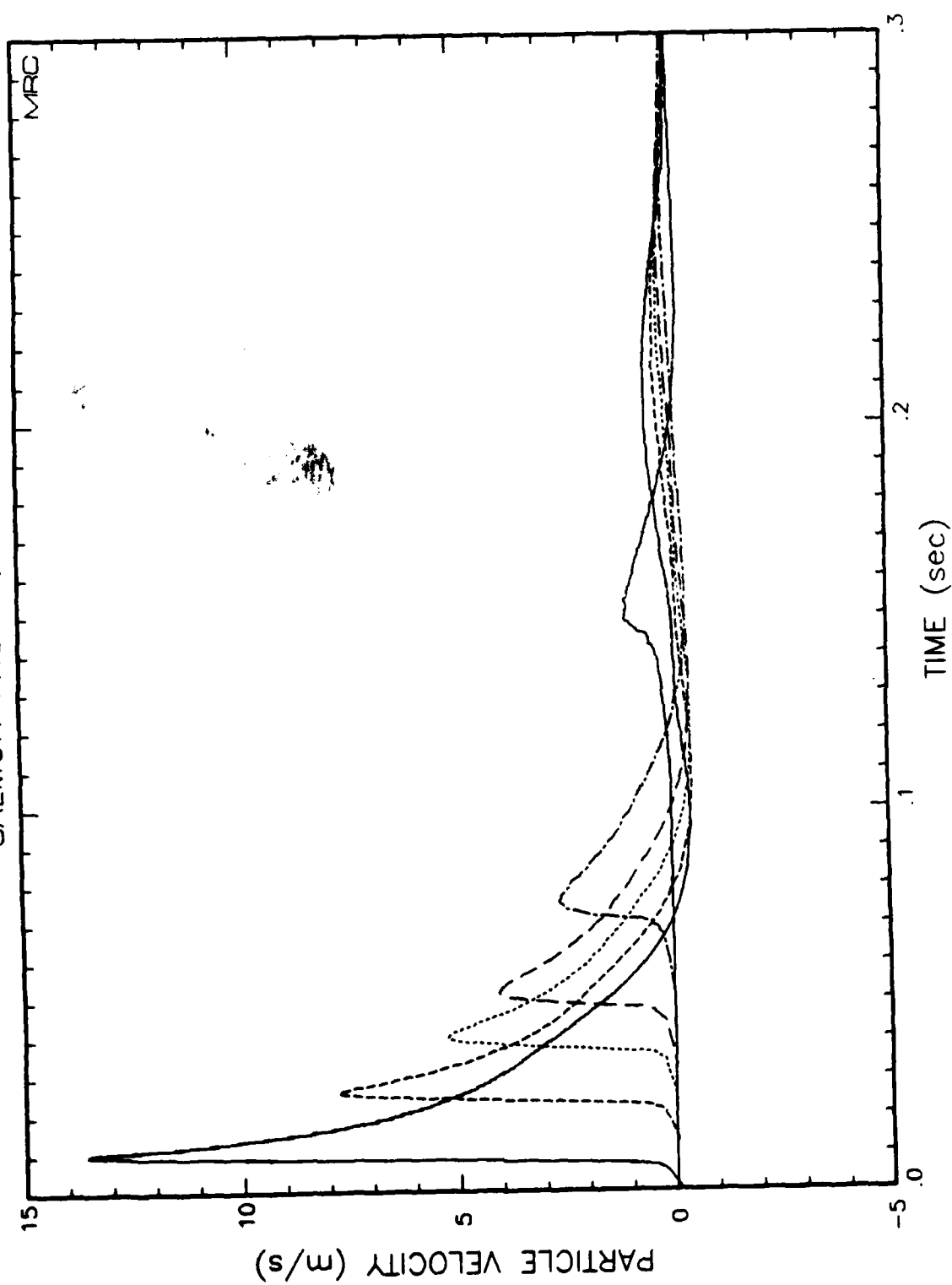


Figure 7. Calculated pulses at Salmon ranges for smoothed shear failure and  $Q=10$ .

## SECTION 4

### COMMENTS

This work indicates that the elastic precursor or leading toe seen in Salmon near-field, moderate strain, velocity data is reproduced rather well with the hypothesis of partial shear failure which is activated for the duration of the pulse when the compressional strain exceeds  $10^{-4}$ . This also gives an attenuation mechanism which accounts for much of the energy loss seen in the decay of pulses from Salmon with range. However, the overall attenuation produced is not quite adequate to account for that seen in the data. The addition of a linear absorption band attenuation, which is active over much of the significant frequency range appropriate to Salmon and which has a  $Q$  of 10, then provides a propagation model which nearly reproduces the signals at ranges beyond 166 meters when the observed signal at this range is used as the source. Furthermore, this threshold mechanism provides a transition to more modest attenuation at small strains which is required to be consistent with Cowboy data. While there is no assurance that this mechanism applies in other than the salt medium, Perret points out that "elastic precursors" of a similar character have been seen in UGT pulses in both alluvium and dolomite.

In addition to accounting for much of the Salmon data, the shear failure mechanism also, when applied to different yield events in salt, will produce simple scaling as observed over a wide range of explosive events.

The fact that the reduction in compressional wave speed is attributed to shear failure, rather than alteration of some other material property, is largely a matter of consistency with past thinking on modes of material behavior; there is no direct experimental link to shear properties. The general agreement with data which results here could just as well have been produced by any method which reduces the compressional modulus in the required amount.

The fact that the NER experiments give an apparently linear  $Q$  of about 20 for small strains of  $10^{-6}$  while Sterling data at comparable strains have much larger  $Q$  is a matter of some concern. However it is known that the attenuation of a material can be a strong function of the liquid content. Spencer<sup>20</sup> made a series of attenuation measurements in several types of rock in dry and water saturated states. He found that dry rocks tend to show only modest attenuation while the water saturated samples had minimum  $Q$ 's of from 4 in sandstone to about 40 in limestone. He found that the attenuation for saturated rocks is quite frequency dependent with peaks at 10 to 1000



Hz depending on the material. He further found that the attenuation spectrum is consistent with dispersion in the modulus so that the mechanism is apparently linear. This sort of result indicates that much care must be taken in comparing experimental results taken for different levels of water saturation and at different frequencies even when strain levels are quite low.

There is a second area where different experiments appear to yield different results. The work of Tittmann on decaying oscillations of salt and other bars give apparent nonlinear behavior but they also show very mild attenuation in the linear regime. As observed by Coyner, the attenuation from these multiple cycle experiments seem to be consistently much less than from propagation (single pulse) experiments at comparable strains and frequencies or from hysteresis loop experiments. For nonlinear attenuation, there does not need to be any particular relation between the effective  $Q$  from pulse and oscillatory experiments - the detailed nature of the mechanism must be known to relate these. For the example of partial shear failure, multiple cycle experiments will produce very small attenuation estimates since all the failure will take place by the time a single cycle has been completed - after that only the intrinsic attenuation will be active.

It should be emphasized that the use of a  $Q$  description for attenuation which is clearly nonlinear is probably not useful, except as a crude estimate of the degree of amplitude reduction. In fact, the use of  $Q$  in nonlinear cases can provide very deceptive results since the frequency and range dependence are generally mixed. It would be best to describe the attenuation mechanism directly in terms of an equation of state. This will allow the application to different experiments. Put another way, the result of a nonlinear attenuation for a propagation experiment can always be used to find an effective  $Q$  by, say, use of spectral ratios but the same mechanism will produce a different effective  $Q$  if the character of the initial waveform is changed. The effective  $Q$  is not a robust quantity for nonlinear attenuation.

We expect to use the finite difference propagation code, which was developed as a tool for our current work on Salmon, as a testbed for development of nonlinear constitutive relations. This avoids the use of  $Q$  and concentrates directly on the physical mechanisms which produce attenuation. Ideally one would like to express a constitutive relation in terms of parameters known to be important, such as porosity, effective stress, crack density, crack growth, etc., in order to allow a model which can be generalized to different media.

## REFERENCES

1. Examples of such considerations are: Mueller, R.A. and J.R. Murphy, *Seismic Characteristics of Underground Nuclear Detonations*, Bull. Seis. Soc. Am., 61, 1975, 1971; and Murphy, J.R., *Seismic Coupling and Magnitude/Yield Relations for Underground Nuclear Detonations in Salt, Granite, Tuff/Rhyolite and Shale Emplacement Media*, CSC-TR-77-0004, Computer Sciences Corporation, 1977.
2. Cherry, J.T., N. Rimer, W.O. Wray, *Seismic Coupling from a Nuclear Explosion: The Dependence of the Reduced Displacement Potential on the Nonlinear Behavior of the Near Source Rock Environment*, SSS-R-76-2742, Systems, Science and Software, Sept 1975.
3. Riney, T.D., et al., *Constitutive Models and Computer Techniques for Ground Motion Predictions*, DNA 3180F, Systems, Science and Software, March 1973.
4. Cherry, J.T., N. Rimer, W.O. Wray, *Verification of the Effective Stress and Air Void Porosity Constitutive Models*, VSC-TR-83-1, S-CUBED, August 1982.
5. Perret, W.R., *Free-Field Particle Motion from A Nuclear Explosion in Salt, Part I, Project Dribble, Salmon Event*, VUF-3012, Sandia, 1967.
6. Rogers, L.A., *Free-Field Motion Near a Nuclear Explosion in Salt: Project Salmon*, J. Geophys. Res. 71, 3425 (1966).
7. McCartor, G., and W. Wortman, *Experimental and Analytic Characterization of Nonlinear Seismic Attenuation*, MRC-R-900, Mission Research Corp., March 1985.
8. McLaughlin, K.L. and I.N. Gupta, *Strain and Frequency Dependent Attenuation Estimates in Salt from Salmon and Sterling Near-Field Data*, Teledyne Geotech, to be submitted to Geophysical Research Letters, 1986.
9. Murphy, J.R., *A Review of Available Free-Field Seismic Data from Underground Nuclear Explosives in Salt and Granite*, CSC-TR-78-0003, Computer Sciences Corporation, September 1978.
10. Trulio, J., Applied Theory, Inc., private communications, 1986.
11. Murphey, B.F., *Particle Motions Near Explosions in Halite*, J. Geophys. Res. 66, 947 (1961).
12. Minster, J.B. and S.M. Day, *Decay of Wave Fields Near an Explosive Source Due to High-Strain Nonlinear Attenuation*, J. Geophys. Res. 91, 2113 (1986).

13. Wortman, W. and G. McCartor, *Nonlinear Seismic Attenuation from Cowboy and Other Explosive Sources*, MRC-R-1107, Mission Research Corp., September 1987.
14. Larson, D.B., *Inelastic Wave Propagation in Sodium Chloride*, Bull. Seism. Soc. Am. 72, 2107 (1982).
15. Tittmann, B.R., *Non-Linear Wave Propagation Study*, SC5361.3SAR, Rockwell International Science Center, 1983.
16. Coyner, K.B., *Attenuation Measurements on Dry Sierra White Granite, Dome Salt and Berea Sandstone*, New England Research, September 1987.
17. Trulio, J., *Simple Scaling and Nuclear Monitoring*, ATR-78-45-1, Applied Theory, Inc., 1978.
18. Ahrens, T.J. and G.E. Duvall, *Stress Relaxation behind Elastic Shock Waves in Rocks*, J. Geophys. Res. 71, 4349 (1966).
19. Taylor, J.W. and M.H. Rice, *Elastic-Plastic Properties of Iron*, J. Appl. Phys. 34, 364 (1963).
20. Spencer, J.W., Jr., *Stress Relaxations at Low Frequencies in Fluid-Saturated Rocks: Attenuation and Modulus Dispersion*, J. Geophys. Res. 86, 1803 (1981).

## APPENDIX A

### WILKINS FINITE DIFFERENCE EQUATIONS

The difference method used to solve for the spherical propagation of a pulse is based on that given by Wilkins.<sup>1</sup> The essential features of this approach are as follows:

The equation of motion is

$$\frac{\rho^0 \dot{U}}{V} = \frac{\partial \Sigma_r}{\partial r} + 2 \frac{\Sigma_r - \Sigma_0}{r} \quad (\text{A} - 1)$$

where the principal stresses are

$$\Sigma_r = -(P + q) + s_1 \quad (\text{A-2})$$

$$\Sigma_\theta = -(P + q) + s_2 \quad (\text{A-3})$$

in terms of the hydrostatic pressure,  $P$ , the artificial viscous pressure,  $q$ , and the stress deviators. The reference density is  $\rho^0$ , the relative volume is  $V$  and  $U$  is the particle velocity.

The continuity equation is

$$\frac{\dot{V}}{V} = \frac{1}{r^2} \frac{\partial(r^2 U)}{\partial r} \quad (\text{A} - 4)$$

where  $r$  is spherical radial position.

The energy equation is

$$\dot{E} - V[s_1 \dot{\epsilon}_1 + 2s_2 \dot{\epsilon}_2] + (P + q)\dot{V} = 0 \quad (\text{A} - 5)$$

where  $E$  is the internal energy and  $\epsilon$  are strains:

$$\dot{\epsilon}_1 = \partial U / \partial r \quad (\text{A-6})$$

$$\dot{\epsilon}_2 = U/r \quad (\text{A-7})$$

Artificial viscous pressure is taken from Viscelli's<sup>2</sup> work as:

$$q = C_L \frac{\rho^0 \alpha}{V} \left| \frac{\partial U}{\partial r} \right| \Delta r \quad (\text{A} - 8)$$

where  $C_L$  is a constant (taken as 0.5),  $\alpha$  is the sound speed and  $\Delta r$  is the cell spacing.

For the elastic case the equation of state is

$$\dot{s}_1 = 2\mu(\dot{\epsilon}_1 - \frac{1}{3}\dot{V}/V) \quad (\text{A-9})$$

$$\dot{s}_2 = 2\mu(\dot{\epsilon}_2 - \frac{1}{3}\dot{V}/V) \quad (\text{A-10})$$

$$\dot{P} = -(\lambda + \frac{2}{3}\mu)\dot{V}/V \quad (\text{A-11})$$

where  $\lambda$  and  $\mu$  are the Lamé elastic constants ( $\lambda + \frac{2}{3}\mu$  is the bulk modulus).

The finite difference version equations is taken by division of the material into  $N$  mass intervals

$$m_{j+\frac{1}{2}} = \frac{\rho^0}{3V^0} \left( \frac{(r_{j+1}^0)^3 - (r_j^0)^3}{d} \right) \quad j = 1, \dots, N \quad (\text{A} - 12)$$

The equation of motion for the velocity for the  $j^{\text{th}}$  element at the  $n^{\text{th}}$  time

$$U_j^{n+1} = U_j^{n-\frac{1}{2}} + \frac{\Delta t^n}{\phi_j^n} [(\Sigma_r)_n^{j+\frac{1}{2}} - (\Sigma_r)_n^{j-\frac{1}{2}}] + 2\Delta t^n(\beta_j^n) \quad (\text{A} - 13)$$

where

$$(\Sigma_r)_n^{j+\frac{1}{2}} = \left\{ - (P^n + q^{n-\frac{1}{2}}) + s_1^n \right\}_{j+\frac{1}{2}} \quad (\text{A-14})$$

$$(\Sigma_\theta)_n^{j+\frac{1}{2}} = \left\{ - (P^n + q^{n-\frac{1}{2}}) + s_2^n \right\}_{j+\frac{1}{2}} \quad (\text{A-15})$$

and

$$\phi_j^n = \frac{1}{2} \left[ \rho_{j+\frac{1}{2}}^0 \left( \frac{r_{j+1}^n - r_j^n}{V_{j+\frac{1}{2}}^n} \right) + \rho_{j-\frac{1}{2}}^0 \left( \frac{r_j^n - r_{j-1}^n}{V_{j-\frac{1}{2}}^n} \right) \right] \quad (\text{A-16})$$

$$\beta_j^n = \frac{1}{2} \left\{ \left[ \frac{(\Sigma_r)_n^{j+\frac{1}{2}} - (\Sigma_\theta)_n^{j+\frac{1}{2}}}{\frac{1}{2}(r_{j+1}^n + r_j^n)} \right] \left( \frac{V^n}{\rho^0} \right)_{j+\frac{1}{2}} + \left[ \frac{(\Sigma_r)_n^{j+\frac{1}{2}} - (\Sigma_\theta)_n^{j+\frac{1}{2}}}{\frac{1}{2}(r_j^n + r_{j-1}^n)} \right] \left( \frac{V^n}{\rho^0} \right)_{j+\frac{1}{2}} \right\} \quad (\text{A-17})$$

At an outside regional boundary J

$$\phi_J^n = \frac{1}{2} \rho_{J-\frac{1}{2}}^0 \left( \frac{r_J^n - r_{J-1}^n}{V_{J-\frac{1}{2}}^n} \right) \quad (\text{A-18})$$

$$\beta_J^n = \left[ \frac{(\Sigma_r)_{J-\frac{1}{2}}^n - (\Sigma_\theta)_{J-\frac{1}{2}}^n}{\frac{1}{2}(r_J^n + r_{J-1}^n)} \right] \left( \frac{V_n}{\rho_0} \right)_{J-\frac{1}{2}} \quad (\text{A-19})$$

while at an inside regional boundary

$$\phi_J^n = \frac{1}{2} \rho_{J+\frac{1}{2}}^0 \left( \frac{r_J^n - r_{J+1}^n}{V_{J+\frac{1}{2}}^n} \right) \quad (\text{A-20})$$

$$\beta_J^n = \left[ \frac{(\Sigma_r)_{J+\frac{1}{2}}^n - (\Sigma_\theta)_{J+\frac{1}{2}}^n}{\frac{1}{2}(r_J^n + r_{J+1}^n)} \right] \left( \frac{V_n}{\rho_0} \right)_{J+\frac{1}{2}} \quad (\text{A-21})$$

Given the velocity, the positions are advanced by

$$r_j^{n+1} = r_j^n + U_j^{n+\frac{1}{2}} \Delta t^{n+\frac{1}{2}} \quad (\text{A-22})$$

The equation of continuity is

$$V_{j+\frac{1}{2}}^{n+1} = V_{j+\frac{1}{2}}^n + \Delta t^{n+\frac{1}{2}} \left( \frac{\rho^0}{m} \right)_{j+\frac{1}{2}} \left[ U_{j+1}^{n+\frac{1}{2}} \left( r_{j+1}^{n+\frac{1}{2}} \right)^2 - U_j^{n+\frac{1}{2}} \left( r_j^{n+\frac{1}{2}} \right)^2 + \chi_{j+\frac{1}{2}}^{n+\frac{1}{2}} \right] \quad (\text{A-23})$$

with

$$\eta_{j+\frac{1}{2}}^{n+1} = \frac{1}{V_{j+\frac{1}{2}}^{n+1}} \quad (\text{A-24})$$

where

$$r_{j+1}^{n+\frac{1}{2}} = \frac{1}{2} (r_{j+1}^{n+1} + r_{j+1}^n) \quad , \text{etc.} \quad (\text{A-25})$$

defines the half time values. And, finally

$$\chi_{j+\frac{1}{2}} = \frac{(\Delta t^{j+\frac{1}{2}})^2}{12} \left[ (U_{j+1}^{n+\frac{1}{2}})^3 - (U_j^{n+\frac{1}{2}})^3 \right] \quad (\text{A} - 26)$$

The strains are defined by

$$(\dot{\epsilon}_1)_{j+\frac{1}{2}}^{n+\frac{1}{2}} = \frac{U_{j+1}^{n+\frac{1}{2}} - U_j^{n+\frac{1}{2}}}{r_{j+1}^{n+\frac{1}{2}} - r_j^{n+\frac{1}{2}}} \quad (\text{A-27})$$

$$(\dot{\epsilon}_2)_{j+\frac{1}{2}}^{n+\frac{1}{2}} = \frac{U_{j+1}^{n+\frac{1}{2}} + U_j^{n+\frac{1}{2}}}{r_{j+1}^{n+\frac{1}{2}} + r_j^{n+\frac{1}{2}}} \quad (\text{A-28})$$

and the stress deviators are advanced by

$$(s_1)_{j+\frac{1}{2}}^{n+1} = (s_1)_{j+\frac{1}{2}}^n + 2\mu \left[ (\dot{\epsilon}_1)_{j+\frac{1}{2}}^{n+\frac{1}{2}} \Delta t^{n+\frac{1}{2}} - \frac{1}{3} \left( \frac{V^{n+1} - V^n}{V^{n+\frac{1}{2}}} \right)_{j+\frac{1}{2}} \right] \quad (\text{A-29})$$

$$(s_2)_{j+\frac{1}{2}}^{n+1} = (s_2)_{j+\frac{1}{2}}^n + 2\mu \left[ (\dot{\epsilon}_2)_{j+\frac{1}{2}}^{n+\frac{1}{2}} \Delta t^{n+\frac{1}{2}} - \frac{1}{3} \left( \frac{V^{n+1} - V^n}{V^{n+\frac{1}{2}}} \right)_{j+\frac{1}{2}} \right] \quad (\text{A-30})$$

Artificial viscous pressure is included by

$$q_{j+\frac{1}{2}}^{n+\frac{1}{2}} = C_L \alpha \rho^0 \eta_{j+\frac{1}{2}}^{n+\frac{1}{2}} \left| U_{j+1}^{n+\frac{1}{2}} - U_j^{n+\frac{1}{2}} \right| \quad ; \quad (\text{A} - 31)$$

where  $C_L \approx 0.5$  (constant) and  $\alpha$  in the compressional wave speed.

The energy equation is advanced by

$$(E_1)_{j+\frac{1}{2}}^{n+1} = (E_1)_{j+\frac{1}{2}}^n + V_{j+\frac{1}{2}}^{n+\frac{1}{2}} (s_1)_{j+\frac{1}{2}}^{n+\frac{1}{2}} (\dot{\epsilon}_1)_{j+\frac{1}{2}}^{n+\frac{1}{2}} \Delta t^{n+\frac{1}{2}} \quad (\text{A-32})$$

$$(E_2)_{j+\frac{1}{2}}^{n+1} = (E_2)_{j+\frac{1}{2}}^n + 2V_{j+\frac{1}{2}}^{n+\frac{1}{2}} (s_2)_{j+\frac{1}{2}}^{n+\frac{1}{2}} (\dot{\epsilon}_2)_{j+\frac{1}{2}}^{n+\frac{1}{2}} \Delta t^{n+\frac{1}{2}} \quad (\text{A-33})$$

$$(E_1)_{j+\frac{1}{2}}^{n+1} = \left\{ E_1^n - \left\{ \frac{1}{2} [P^{n+1} + P^n] + q^{n+\frac{1}{2}} \right\} \cdot [V^{n+1} - V^n] + \Delta E_1 + \Delta E_2 \right\}_{j+\frac{1}{2}} \quad (\text{A-34})$$

For the current application, this energy is just a diagnostic and is not fed back through any equation of state.

The hydrostatic pressure for the elastic case is

$$P_{j+\frac{1}{2}}^{n+1} = \left( \lambda + \frac{2}{3}\mu \right) \left( \eta_{j+\frac{1}{2}}^{n+1} - 1 \right) \quad (\text{A} - 35)$$

## REFERENCES

1. Wilkins, M.L., "Calculation of Elastic-Plastic Flow," *Methods in Computational Physics*, Vol. 3, 1964.
2. Viecelli, J.A., "The Linear Q and the Calculation of Decaying Spherical Shocks in Solids," *J. Comp. Phys.*, 12, 187 (1973).



## APPENDIX B

### INCLUSION OF DAY-MINSTER Q IN FINITE DIFFERENCES

Day and Minster<sup>1</sup> have shown how to include an arbitrary linear Q function in time stepping calculations. For an absorption band an analytic solution is available. An outline of their methods, as easily generalized to the spherical case is given here.

For a single normalized relaxation function,  $m(t)$ , the stresses and strains are related by

$$\Sigma_r = (\lambda + 2\mu) \int m(t - \tau) \epsilon_1(\tau) d\tau + 2\lambda \int m(t - \tau) \epsilon_2(\tau) d\tau \quad (B-1)$$

$$\Sigma_\theta = (2\lambda + 2\mu) \int m(t - \tau) \epsilon_2(\tau) d\tau + \lambda \int m(t - \tau) \epsilon_1(\tau) d\tau \quad (B-2)$$

Here the strains are

$$\epsilon_1 = \frac{\partial u}{\partial r} \quad (B-3)$$

$$\epsilon_2 = \frac{u}{r} \quad (B-4)$$

where  $u$  is displacement. Generally one could have two different relaxation functions (e.g., bulk and shear) but we shall not consider this possibility. The  $\lambda$  and  $\mu$  are the usual Lamé constants which are now the unrelaxed or high frequency moduli of the medium. The stresses can be written in terms of Q corrected strains,  $e$ , as

$$\Sigma_r = (\lambda + 2\mu)e_1 + 2\lambda e_2 \quad (B-5)$$

$$\Sigma_\theta = (2\lambda + 2\mu)e_2 + \lambda e_1 \quad (B-6)$$

Day and Minster have shown how to express the  $e_i$  in terms of the  $\epsilon_i$

$$e_i = \int m(t - \tau) \epsilon_i d\tau \quad (B-7)$$

using a sequence of  $m$  Padé approximants to write the integral relation as a differential relation. For an absorption band attenuation with relaxation times between  $\tau_1$  and  $\tau_2$  and with a flat spectrum they show that the integral relation can be replaced by

$$e_i(t) = \epsilon_i(t) - \sum_{k=1}^m \zeta_i^k(t) \quad (B-8)$$

where

$$\frac{d}{dt} \zeta_i^k + \nu_k \zeta_i^k = \left( \frac{\tau_1^{-1} - \tau_2^{-1}}{\pi} W_k Q_0^{-1} \right) \epsilon_i(t) \quad k=1, \dots, m \quad (B-9)$$

Here  $Q_0$  is the target  $Q$  in the absorption band, the

$$\nu_k = \frac{1}{2} [\ell_k(\tau_1^{-1} - \tau_2^{-1}) + (\tau_1^{-1} + \tau_2^{-1})] \quad (B-10)$$

where the  $\ell_k$  are the abscissas and  $W_k$  are the weights for  $m$ -point Gauss-Legendre quadrature. The index  $m$  is that of the Padé approximant. As  $m$  increases, the solution converges to the analytic result which in the frequency domain is

$$i\omega \tilde{m}(\omega) = \tilde{m}(\omega) = 1 - \frac{2}{\pi Q_0} \ell_n \left[ \frac{\tau_2}{\tau_1} \left( \frac{1 + \omega^2 \tau_1^2}{1 + \omega^2 \tau_2^2} \right)^{1/2} \right] + \frac{2i}{\pi Q_0} \tan^{-1} \left( \frac{\omega(\tau_2 - \tau_1)}{1 + \omega^2 \tau_1 \tau_2} \right) \quad (B-11)$$

The convergence of the sequence with increasing  $m$  is shown in Figure B-1. For calculations given in the main text  $m=5$  was used since convergence is near. Use of significantly larger  $m$  slows down the calculations of pulse propagation since each  $m$  adds an additional differential equation which must be carried. In finite difference form the  $\zeta$  are advanced for both  $i$  by

$$(\zeta^k)_{j+\frac{1}{2}}^{n+\frac{1}{2}} = \left( \frac{2 - \Delta t^n \nu_k}{2 + \Delta t^n \nu_k} \right) (\zeta^k)_{j+\frac{1}{2}}^{n-\frac{1}{2}} + \left( \frac{\Delta t^n}{2 + \Delta t^n \nu_k} \frac{\tau_1^{-1} - \tau_2^{-1}}{\pi Q_0} W_k \right) (\epsilon_{j+\frac{1}{2}}^{n+\frac{1}{2}} + \epsilon_{j+\frac{1}{2}}^{n-\frac{1}{2}}) \quad (B-12)$$

and then the

$$\dot{\epsilon} = \dot{\epsilon} - \sum_{k=1}^m \dot{\zeta}_k \quad (B-13)$$

These are then used to advance the stresses by

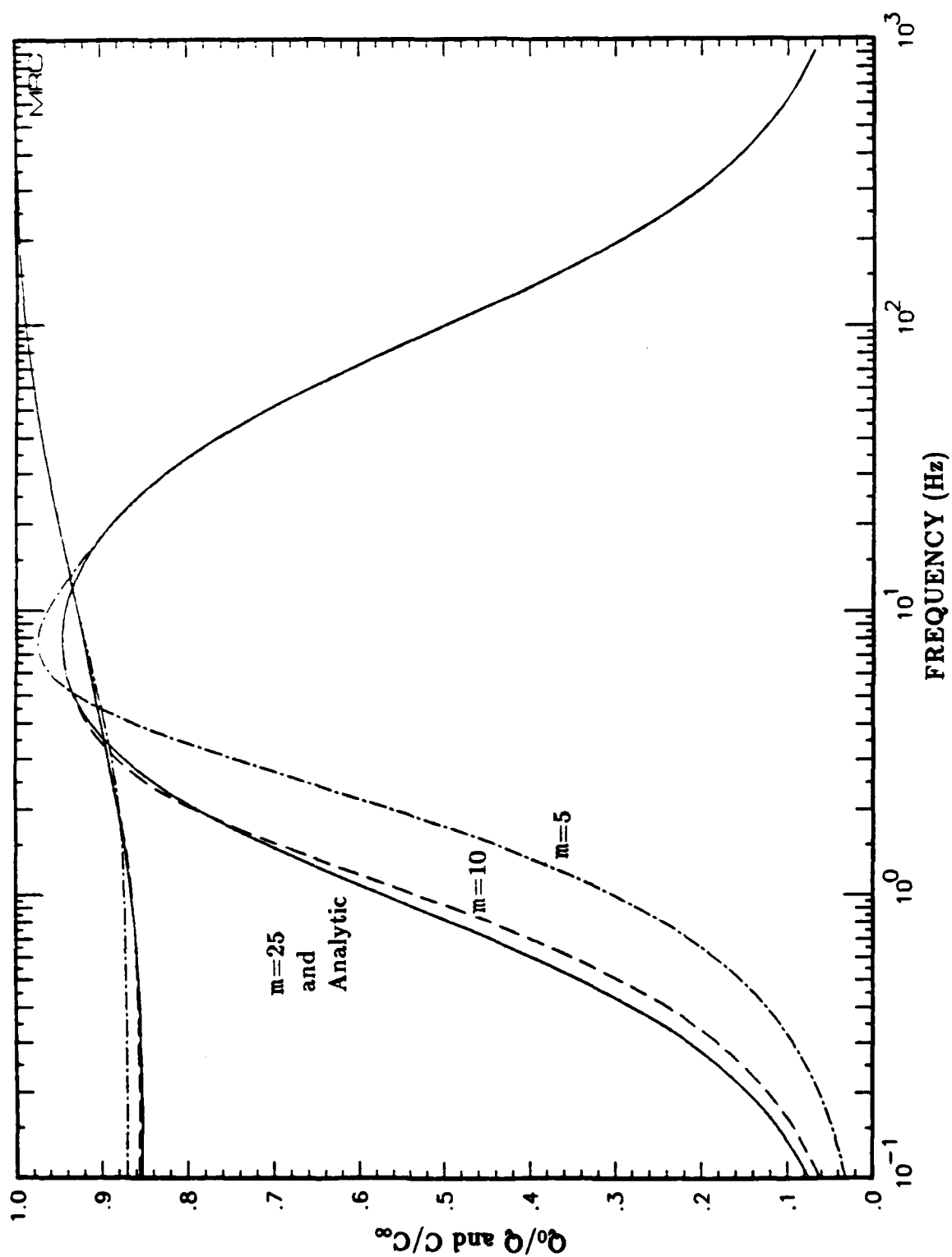


**Figure B-1.** Absorption band  $Q$  and propagation speed  $C$  for three values of the Padé index  $m$  for  $Q_0 = 20$ ,  $\tau_1 = 1.59 \times 10^{-3}$  and  $\tau_2 = 1.59 \times 10^{-1}$ .

$$\dot{s}_1 = \frac{4}{3}\mu(\dot{e}_1 - \dot{e}_2) \quad (B-14)$$

$$\dot{P} = (\lambda + \frac{2}{3}\mu)(\dot{e}_1 + 2\dot{e}_2) \quad (B-15)$$

so

$$(s_1)_{j+\frac{1}{2}}^{n+1} = (s_1)_{j+\frac{1}{2}}^n + \Delta t^{n+\frac{1}{2}}(\dot{s}_1)_{j+\frac{1}{2}}^n \quad (B-16)$$

$$P_{j+\frac{1}{2}}^{n+1} = P_{j+\frac{1}{2}}^n + \Delta t^{n+\frac{1}{2}}\dot{P}_{j+\frac{1}{2}}^n \quad (B-17)$$

$$(s_2)_{j+\frac{1}{2}}^{n+1} = \frac{1}{2}(s_1)_{j+\frac{1}{2}}^{n+1} \quad (B-18)$$

are used in place of the procedure applied in Appendix A.

#### REFERENCE

1. Day, S.M. and J.B. Minster, *Numerical Simulation of Attenuated Wavefields Using a Padé Approximant Method*, Geophys. J.R. Astr. Soc. 78, 105 (1984).

CONTRACTORS (United States)

Professor Keiliti Aki  
Center for Earth Sciences  
University of Southern California  
University Park  
Los Angeles, CA 90089-0741

Professor Charles B. Archambeau  
Cooperative Institute for Resch  
in Environmental Sciences  
University of Colorado  
Boulder, CO 80309

Dr. Thomas C. Bache Jr.  
Science Applications Int'l Corp.  
10210 Campus Point Drive  
San Diego, CA 92121 (2 copies)

Dr. Muawia Barazangi  
Institute for the Study of the  
Continent  
SNEE Hall  
Cornell University  
Ithaca, NY 14853

Dr. Douglas R. Baumgardt  
Signal Analysis & Systems Div.  
ENSCO, Inc.  
5400 Port Royal Road  
Springfield, VA 22151-2388

Dr. Jonathan Berger  
Institute of Geophysics and  
Planetary Physics  
Scripps Institution of Oceanography  
A-025  
University of California, San Diego  
La Jolla, CA 92093

Dr. S. Bratt  
Science Applications Int'l Corp.  
10210 Campus Point Drive  
San Diego, CA 92121

Dr. Lawrence J. Burdick  
Woodward-Clyde Consultants  
P.O. Box 93245  
Pasadena, CA 91109-3245 (2 copies)

Professor Robert W. Clayton  
Seismological Laboratory/Div. of  
Geological & Planetary Sciences  
California Institute of Technology  
Pasadena, CA 91125

Dr Karl Coyner  
N. E. Research, Inc.  
76 Olcott Drive  
White River Junction, VT 05001

Dr. Steven Day  
Dept. of Geological Sciences  
San Diego State U.  
San Diego, CA 92182

Dr. Zoltan A. Der  
ENSCO, Inc.  
5400 Port Royal Road  
Springfield, VA 22151-2388

Professor John Ferguson  
Center for Lithospheric Studies  
The University of Texas at Dallas  
P.O. Box 830688  
Richardson, TX 75083-0688

Professor Stanley Flatte'  
Applied Sciences Building  
University of California,  
Santa Cruz, CA 95064

Dr. Alexander Florence  
SRI International  
333 Ravenswood Avenue  
Menlo Park, CA 94025-3493

Professor Steven Grand  
Department of Geology  
245 Natural History Building  
1301 West Green Street  
Urbana, IL 61801

Dr. Henry L. Gray  
Associate Dean of Dedman College  
Department of Statistical Sciences  
Southern Methodist University  
Dallas, TX 75275

Professor Roy Greenfield  
Geosciences Department  
403 Deike Building  
The Pennsylvania State University  
University Park, PA 16802

Professor David G. Harkrider  
Seismological Laboratory  
Div of Geological & Planetary Sciences  
California Institute of Technology  
Pasadena, CA 91125

Dr. Vernon F. Cormier  
Department of Geology & Geophysics  
U-45, Room 207  
The University of Connecticut  
Storrs, Connecticut 06268

Professor Eugene Herrin  
Institute for the Study of Earth  
and Man/Geophysical Laboratory  
Southern Methodist University  
Dallas, TX 75275

Professor Robert B. Herrmann  
Department of Earth & Atmospheric  
Sciences  
Saint Louis University  
Saint Louis, MO 63156

Professor Bryan Isacks  
Cornell University  
Dept of Geological Sciences  
SNEE Hall  
Ithaca, NY 14850

Professor Lane R. Johnson  
Seismographic Station  
University of California  
Berkeley, CA 94720

Professor Thomas H. Jordan  
Department of Earth, Atmospheric  
and Planetary Sciences  
Mass Institute of Technology  
Cambridge, MA 02139

Dr. Alan Kafka  
Department of Geology &  
Geophysics  
Boston College  
Chestnut Hill, MA 02167

Professor Leon Knopoff  
University of California  
Institute of Geophysics  
& Planetary Physics  
Los Angeles, CA 90024

Professor Charles A. Langston  
Geosciences Department  
403 Deike Building  
The Pennsylvania State University  
University Park, PA 16802

Professor Donald V. Helmberger  
Seismological Laboratory  
Div of Geological & Planetary Sciences  
California Institute of Technology  
Pasadena, CA 91125

Dr. Gary McCartor  
Mission Research Corp.  
735 State Street  
P.O. Drawer 719  
Santa Barbara, CA 93102 (2 copies)

Professor Thomas V. McEvilly  
Seismographic Station  
University of California  
Berkeley, CA 94720

Dr. Keith L. McLaughlin  
S-CUBED,  
A Division of Maxwell Laboratory  
P.O. Box 1620  
La Jolla, CA 92038-1620

Professor William Menke  
Lamont-Doherty Geological Observatory  
of Columbia University  
Palisades, NY 10964

Professor Brian J. Mitchell  
Department of Earth & Atmospheric  
Sciences  
Saint Louis University  
Saint Louis, MO 63156

Mr. Jack Murphy  
S-CUBED  
A Division of Maxwell Laboratory  
11800 Sunrise Valley Drive  
Suite 1212  
Reston, VA 22091 (2 copies)

Professor J. A. Orcutt  
Institute of Geophysics and Planetary  
Physics, A-205  
Scripps Institute of Oceanography  
Univ. of California, San Diego  
La Jolla, CA 92093

Professor Keith Priestley  
University of Nevada  
Mackay School of Mines  
Reno, NV 89557

Professor Thorne Lay  
Department of Geological Sciences  
1006 C.C. Little Building  
University of Michigan  
Ann Arbor, MI 48109-1063

Dr. Randolph Martin III  
New England Research, Inc.  
76 Olcott Drive  
White River Junction, VT 05001

Dr. Alan S. Ryall, Jr.  
Center of Seismic Studies  
1300 North 17th Street  
Suite 1450  
Arlington, VA 22209-2308 (4 copies)

Professor Charles C. Sammis  
Center for Earth Sciences  
University of Southern California  
University Park  
Los Angeles, CA 90089-0741

Professor Christopher H. Scholz  
Geological Sciences  
Lamont-Doherty Geological Observatory  
Palisades, NY 10964

Dr. Jeffrey L. Stevens  
S-CUBED,  
A Division of Maxwell Laboratory  
P.O. Box 1620  
La Jolla, CA 92038-1620

Professor Brian Stump  
Institute for the Study of Earth & Man  
Geophysical Laboratory  
Southern Methodist University  
Dallas, TX 75275

Professor Ta-liang Teng  
Center for Earth Sciences  
University of Southern California  
University Park  
Los Angeles, CA 90089-0741

Professor Paul G. Richards  
Lamont-Doherty Geological  
Observatory of Columbia Univ.  
Palisades, NY 10964

Wilmer Rivers  
Teledyne Geotech  
314 Montgomery Street  
Alexandria, VA 22314

Dr. Clifford Thurber  
State University of New York at  
Stony Brooks  
Dept of Earth and Space Sciences  
Stony Brook, NY 11794-2100

Professor M. Nafi Toksoz  
Earth Resources Lab  
Dept of Earth, Atmospheric and  
Planetary Sciences  
Massachusetts Institute of Technology  
42 Carleton Street  
Cambridge, MA 02142

Professor Terry C. Wallace  
Department of Geosciences  
Building #77  
University of Arizona  
Tucson, AZ 85721

Weidlinger Associates  
ATTN: Dr. Gregory Wojcik  
4410 El Camino Real, Suite 110  
Los Altos, CA 94022

Professor Francis T. Wu  
Department of Geological Sciences  
State University of New York  
at Binghamton  
Vestal, NY 13901

OTHERS (United States)

Dr. Monem Abdel-Gawad  
Rockwell Internat'l Science Center  
1049 Camino Dos Rios  
Thousand Oaks, CA 91360

Professor Shelton S. Alexander  
Geosciences Department  
403 Deike Building  
The Pennsylvania State University  
University Park, PA 16802

Dr. Ralph Archuleta  
Department of Geological  
Sciences  
Univ. of California at  
Santa Barbara  
Santa Barbara, CA

J. Barker  
Department of Geological Sciences  
State University of New York  
at Binghamton  
Vestal, NY 13901

Mr. William J. Best  
907 Westwood Drive  
Vienna, VA 22180

Dr. N. Biswas  
Geophysical Institute  
University of Alaska  
Fairbanks, AK 99701

Dr. G. A. Bollinger  
Department of Geological Sciences  
Virginia Polytechnical Institute  
21044 Derring Hall  
Blacksburg, VA 24061

Dr. James Bulau  
Rockwell Int'l Science Center  
1049 Camino Dos Rios  
P.O. Box 1085  
Thousand Oaks, CA 91360

Mr. Roy Burger  
1221 Serry Rd.  
Schenectady, NY 12309

Dr. Robert Burridge  
Schlumberger-Doll Resch Ctr.  
Old Quarry Road  
Ridgefield, CT 06877

Science Horizons, Inc.  
ATTN: Dr. Theodore Cherry  
710 Encinitas Blvd., Suite 101  
Encinitas, CA 92024 (2 copies)

Professor Jon F. Claerbout  
Professor Amos Nur  
Dept. of Geophysics  
Stanford University  
Stanford, CA 94305 (2 copies)

Dr. Anton W. Dainty  
AFGL/LWH  
Hanscom AFB, MA 01731

Professor Adam Dziewonski  
Hoffman Laboratory  
Harvard University  
20 Oxford St.  
Cambridge, MA 02138

Professor John Ebel  
Dept of Geology & Geophysics  
Boston College  
Chestnut Hill, MA 02167

Dr. Donald Forsyth  
Dept. of Geological Sciences  
Brown University  
Providence, RI 02912

Dr. Anthony Gangi  
Texas A&M University  
Department of Geophysics  
College Station, TX 77843

Dr. Freeman Gilbert  
Institute of Geophysics &  
Planetary Physics  
Univ. of California, San Diego  
P.O. Box 109  
La Jolla, CA 92037



Mr. Edward Giller  
Pacific Seirra Research Corp.  
1401 Wilson Boulevard  
Arlington, VA 22209

Dr. Jeffrey W. Given  
Sierra Geophysics  
11255 Kirkland Way  
Kirkland, WA 98033

Rong Song Jih  
Teledyne Geotech  
314 Montgomery Street  
Alexandria, Virginia 22314

Professor F.K. Lamb  
University of Illinois at  
Urbana-Champaign  
Department of Physics  
1110 West Green Street  
Urbana, IL 61801

Dr. Arthur Lerner-Lam  
Lamont-Doherty Geological Observatory  
of Columbia University  
Palisades, NY 10964

Dr. L. Timothy Long  
School of Geophysical Sciences  
Georgia Institute of Technology  
Atlanta, GA 30332

Dr. Peter Malin  
University of California at Santa Barbara  
Institute for Central Studies  
Santa Barbara, CA 93106

Dr. George R. Mellman  
Sierra Geophysics  
11255 Kirkland Way  
Kirkland, WA 98033

Dr. Bernard Minster  
Institute of Geophysics and Planetary  
Physics, A-205  
Scripps Institute of Oceanography  
Univ. of California, San Diego  
La Jolla, CA 92093

Professor John Nabelek  
College of Oceanography  
Oregon State University  
Corvallis, OR 97331

Dr. Geza Nagy  
U. California, San Diego  
Dept of Ames, M.S. B-010  
La Jolla, CA 92093

Dr. Jack Oliver  
Department of Geology  
Cornell University  
Ithaca, NY 14850

Dr. Robert Phinney/Dr. F.A. Dahlen  
Dept of Geological  
Geophysical Sci. University  
Princeton University  
Princeton, NJ 08540 (2 copies)

RADIX Systems, Inc.  
Attn: Dr. Jay Pulli  
2 Taft Court, Suite 203  
Rockville, Maryland 20850

Dr. Norton Rimer  
S-CUBED  
A Division of Maxwell Laboratory  
P.O. 1620  
La Jolla, CA 92038-1620

Professor Larry J. Ruff  
Department of Geological Sciences  
1006 C.C. Little Building  
University of Michigan  
Ann Arbor, MI 48109-1063

Dr. Richard Sailor  
TASC Inc.  
55 Walkers Brook Drive  
Reading, MA 01867

Thomas J. Sereno, Jr.  
Service Application Int'l Corp.  
10210 Campus Point Drive  
San Diego, CA 92121

Dr. David G. Simpson  
Lamont-Doherty Geological Observ.  
of Columbia University  
Palisades, NY 10964

Dr. Bob Smith  
Department of Geophysics  
University of Utah  
1400 East 2nd South  
Salt Lake City, UT 84112

Dr. S. W. Smith  
Geophysics Program  
University of Washington  
Seattle, WA 98195

Dr. Stewart Smith  
IRIS Inc.  
1616 N. Fort Myer Drive  
Suite 1440  
Arlington, VA 22209

Rondout Associates  
ATTN: Dr. George Sutton,  
Dr. Jerry Carter, Dr. Paul Pomeroy  
P.O. Box 224  
Stone Ridge, NY 12484 (4 copies)

Dr. L. Sykes  
Lamont Doherty Geological Observ.  
Columbia University  
Palisades, NY 10964

Dr. Pradeep Talwani  
Department of Geological Sciences  
University of South Carolina  
Columbia, SC 29208

Dr. R. B. Tittmann  
Rockwell International Science Center  
1049 Camino Dos Rios  
P.O. Box 1085  
Thousand Oaks, CA 91360

Professor John H. Woodhouse  
Hoffman Laboratory  
Harvard University  
20 Oxford St.  
Cambridge, MA 02138

Dr. Gregory B. Young  
ENSCO, Inc.  
5400 Port Royal Road  
Springfield, VA 22151-2388

OTHERS (FOREIGN)

Dr. Peter Basham  
Earth Physics Branch  
Geological Survey of Canada  
1 Observatory Crescent  
Ottawa, Ontario  
CANADA K1A 0Y3

Dr. Eduard Berg  
Institute of Geophysics  
University of Hawaii  
Honolulu, HI 96822

Dr. Michel Bouchon - Universite  
Scientifique et Medicale de Grenob  
Lab de Geophysique - Interne et  
Tectonophysique - I.R.I.G.M-B.P.  
38402 St. Martin D'Herès  
Cedex FRANCE

Dr. Hilmar Bungum/NTNF/NORSAR  
P.O. Box 51  
Norwegian Council of Science,  
Industry and Research, NORSAR  
N-2007 Kjeller, NORWAY

Dr. Michel Campillo  
I.R.I.G.M.-B.P. 68  
38402 St. Martin D'Herès  
Cedex, FRANCE

Dr. Kin-Yip Chun  
Geophysics Division  
Physics Department  
University of Toronto  
Ontario, CANADA M5S 1A7

Dr. Alan Douglas  
Ministry of Defense  
Blacknest, Brimpton,  
Reading RG7-4RS  
UNITED KINGDOM

Dr. Manfred Henger  
Fed. Inst. For Geosciences & Nat'l Res.  
Postfach 510153  
D-3000 Hannover 51  
FEDERAL REPUBLIC OF GERMANY

Dr. E. Husebye  
NTNF/NORSAR  
P.O. Box 51  
N-2007 Kjeller, NORWAY

Ms. Eva Johannisson  
Senior Research Officer  
National Defense Research Inst.  
P.O. Box 27322  
S-102 54 Stockholm  
SWEDEN

Tormod Kvaerna  
NTNF/NORSAR  
P.O. Box 51  
N-2007 Kjeller, NORWAY

Mr. Peter Marshall, Procurement  
Executive, Ministry of Defense  
Blacknest, Brimpton,  
Reading RG7-4RS  
UNITED KINGDOM (3 copies)

Dr. Ben Menaheim  
Weizman Institute of Science  
Rehovot, ISRAEL 951729

Dr. Svein Mykkeltveit  
NTNF/NORSAR  
P.O. Box 51  
N-2007 Kjeller, NORWAY (3 copies)

Dr. Robert North  
Geophysics Division  
Geological Survey of Canada  
1 Observatory crescent  
Ottawa, Ontario  
CANADA, K1A 0Y3

Dr. Frode Ringdal  
NTNF/NORSAR  
P.O. Box 51  
N-2007 Kjeller, NORWAY

Dr. Jorg Schlittenhardt  
Federal Inst. for Geosciences & Nat'l Res.  
Postfach 510153  
D-3000 Hannover 51  
FEDERAL REPUBLIC OF GERMANY

University of Hawaii  
Institute of Geophysics  
ATTN: Dr. Daniel Walker  
Honolulu, HI 96822

FOREIGN CONTRACTORS

Dr. Ramon Cabre, S.J.  
Observatorio San Calixto  
Casilla 5939  
La Paz Bolivia

Professor Peter Harjes  
Institute for Geophysik  
Rhur University/Bochum  
P.O. Box 102148, 4630 Bochum 1  
FEDERAL REPUBLIC OF GERMANY

Professor Brian L.N. Kennett  
Research School of Earth Sciences  
Institute of Advanced Studies  
G.P.O. Box 4  
Canberra 2601  
AUSTRALIA

Dr. B. Massinon  
Societe Radiomana  
27, Rue Claude Bernard  
7,005, Paris, FRANCE (2 copies)

Dr. Pierre Mechler  
Societe Radiomana  
27, Rue Claude Bernard  
75005, Paris, FRANCE

GOVERNMENT

Dr. Ralph Alewine III  
DARPA/NMRO  
1400 Wilson Boulevard  
Arlington, VA 22209-2308

Dr. Robert Blandford  
DARPA/NMRO  
1400 Wilson Boulevard  
Arlington, VA 22209-2308

Sandia National Laboratory  
ATTN: Dr. H. B. Durham  
Albuquerque, NM 87185

Dr. Jack Evernden  
USGS-Earthquake Studies  
345 Middlefield Road  
Menlo Park, CA 94025

U.S. Geological Survey  
ATTN: Dr. T. Hanks  
Nat'l Earthquake Resch Center  
345 Middlefield Road  
Menlo Park, CA 94025

Dr. James Hannon  
Lawrence Livermore Nat'l Lab.  
P.O. Box 808  
Livermore, CA 94550

Paul Johnson  
ESS-4, Mail Stop J979  
Los Alamos National Laboratory  
Los Alamos, NM 87545

Ms. Ann Kerr  
DARPA/NMRO  
1400 Wilson Boulevard  
Arlington, VA 22209-2308

Dr. Max Koontz  
US Dept of Energy/DP 5  
Forrestal Building  
1000 Independence Ave.  
Washington, D.C. 20585

Dr. W. H. K. Lee  
USGS  
Office of Earthquakes, Volcanoes,  
& Engineering  
Branch of Seismology  
345 Middlefield Rd  
Menlo Park, CA 94025

Dr. William Leith  
USGS  
Mail Stop 928  
Reston, VA 22092

Dr. Richard Lewis  
Dir. Earthquake Engineering and  
Geophysics  
U.S. Army Corps of Engineers  
Box 631  
Vicksburg, MS 39180

Dr. Robert Masse'  
Box 25046, Mail Stop 967  
Denver Federal Center  
Denver, Colorado 80225

Richard Morrow  
ACDA/VI  
Room 5741  
320 21st Street N.W.  
Washington, D.C. 20451

Dr. Keith K. Nakanishi  
Lawrence Livermore National Lab  
P.O. Box 808, L-205  
Livermore, CA 94550 (2 copies)

Dr. Carl Newton  
Los Alamos National Lab.  
P.O. Box 1663  
Mail Stop C335, Group E553  
Los Alamos, NM 87545

Dr. Kenneth H. Olsen  
Los Alamos Scientific Lab.  
Post Office Box 1663  
Los Alamos, NM 87545

Howard J. Patton  
Lawrence Livermore National  
Laboratory  
P.O. Box 808, L-205  
Livermore, CA 94550

Mr. Chris Paine  
Office of Senator Kennedy  
SR 315  
United States Senate  
Washington, D.C. 20510

AFOSR/NP  
ATTN: Colonel Jerry J. Perrizo  
Bldg 410  
Bolling AFB, Wash D.C. 20332-6448

HQ AFTAC/TT  
Attn: Dr. Frank F. Pilotte  
Patrick AFB, Florida 32925-6001

Mr. Jack Rachlin  
USGS - Geology, Rm 3 C136  
Mail Stop 928 National Center  
Reston, VA 22092

Robert Reinke  
AFWL/NTESG  
Kirtland AFB, NM 87117-6008

HQ AFTAC/TGR  
Attn: Dr. George H. Rothe  
Patrick AFB, Florida 32925-6001

Donald L. Springer  
Lawrence Livermore National Laboratory  
P.O. Box 808, L-205  
Livermore, CA 94550

Dr. Lawrence Turnbull  
OSWR/NED  
Central Intelligence Agency  
CIA, Room 5C48  
Washington, D.C. 20505

Dr. Thomas Weaver  
Los Alamos National Laboratory  
P.O. Box 1663  
MS C335  
Los Alamos, NM 87545

AFGL/SULL  
Research Library  
Hanscom AFB, MA 01731-5000 (2 copies)

Secretary of the Air Force (SAFRD)  
Washington, DC 20330  
Office of the Secretary Defense  
DDR & E  
Washington, DC 20330

DARPA/RMO/Security Office  
1400 Wilson Blvd.  
Arlington, VA 22209

HQ DNA  
ATTN: Technical Library  
Washington, DC 20305

AFGL/XO  
Hanscom AFB, MA 01731-5000

AFGL/LW  
Hanscom AFB, MA 01731-5000

DARPA/PM  
1400 Wilson Boulevard  
Arlington, VA 22209

Defense Technical  
Information Center  
Cameron Station  
Alexandria, VA 22314  
(5 copies)

Defense Intelligence Agency  
Directorate for Scientific &  
Technical Intelligence  
Washington, D.C. 20301

Defense Nuclear Agency/SPSS  
ATTN: Dr. Michael Shore  
6801 Telegraph Road  
Alexandria, VA 22310

AFTAC/CA (STINFO)  
Patrick AFB, FL 32925-6001

Dr. Gregory van der Vink  
Congress of the United States  
Office of Technology Assessment  
Washington, D.C. 20510

Mr. Alfred Lieberman  
ACDA/VI-OA'State Department Building  
Room 5726  
320 - 21st Street, NW  
Washington, D.C. 20451

TACTEC  
Battelle Memorial Institute  
505 King Avenue  
Columbus, OH 43201 (Final report only)

DARPA/RMO/RETRIEVAL  
1400 Wilson Boulevard  
Arlington, VA 22209

END

6-89

DTIC